Human dental pulp stem cells exhibit enhanced properties in comparison to human bone marrow stem cells on neurites outgrowth

Pagella, Pierfrancesco ; Miran, Shayee ; Neto, Estrela ; Martin, Ivan ; Lamghari, Meriem ; Mitsiadis, Thimios A

Abstract: Mesenchymal stem cells (MSCs) have the capacity to self-renew and differentiate into specific cell types and are, therefore, key players during tissue repair and regeneration. The use of MSCs for the regeneration of tissues in vivo is increasingly being explored and already constitutes a promising alternative to existing clinical treatments. MSCs also exert paracrine and trophic functions, including the promotion of innervation that plays fundamental roles in regeneration and in restoration of the function of organs. Human bone marrow stem cells (hBMSCs) and human dental pulp stem cells (hDPSCs) have been used in studies that aimed at the repair and/or regeneration of bone or other tissues of the craniofacial complex. However, the capabilities of hBMSCs and hDPSCs to elicit the growth of specific axons in order to reestablish functional innervation of the healing tissues are not known. Here, we compared the neurotrophic effects of hDPSCs and hBMSCs on trigeminal and dorsal root ganglia neurons using microfluidic organs-on-chips devices. We found that hDPSCs express significantly higher levels of neurotrophins than hBMSCs and consequently neurons cocultured with hDPSCs develop longer axons in the microfluidic co-culture system when compared to neurons cocultured with hBMSCs. Moreover, hDPSCs elicited the formation of extensive axonal networks and established close contacts with neurons, a phenomenon not observed in presence of hBMSCs. Taken together, these findings indicate that hDPSCs constitute a superior option for restoring the functionality of damaged craniofacial tissues, as they are able to support and promote extensive trigeminal innervation.

DOI: https://doi.org/10.1096/fj.201902482r

Human dental pulp stem cells exhibit enhanced properties in comparison to human bone marrow stem cells on neurites outgrowth

Pierfrancesco Pagella[1*], Shayee Miran[1], Estrela Neto[2], Ivan Martin[3], Meriem Lamghari[2], Thimios A. Mitsiadis[1*]

Affiliations:

[1] Orofacial Development and Regeneration, Institute of Oral Biology, Centre of Dental Medicine, University of Zurich, Zurich, Switzerland.

[2] i3S, University of Porto, Porto, Portugal; Institute of Biomedical Engineering (INEB), University of Porto, Porto, Portugal.

[3] Department of Biomedicine, University Hospital Basel, University of Basel, 4031 Basel, Switzerland

***Corresponding authors:** Prof. Thimios A. Mitsiadis, PhD, DDS
Orofacial Development and Regeneration, Institute of Oral Biology, Plattenstrasse 11, 8032 Zurich, Switzerland
Phone: +41 44 63 43390
E-mail: thimios.mitsiadis@zzm.uzh.ch

Pierfrancesco Pagella, PhD
Orofacial Development and Regeneration, Institute of Oral Biology, University of Zurich, Zurich, Switzerland
E-mail: pierfrancesco.pagella@zzm.uzh.ch
Phone: +41 44 63 43306

Keywords: Innervation, trigeminal ganglion, human dental pulp stem cells, human bone marrow stem cells, neurotrophins, microfluidics, organs-on-chips

LIST OF NONSTANDARD ABBREVIATIONS

BDNF	Brain-Derived Neurotrophic Factor
CGRP	Calcitonin Gene Related Peptide
DMEM/F12	Dulbecco's Modified Eagle Medium: Nutrient Mixture F-12
DRG	Dorsal Root Ganglia
FBS	Fetal Bovine Serum
GDNF	Glial-cell Derived Neurotrophic Factor
hBMSC	Human Bone Marrow Stem Cell
hDPSC	Human Dental Pulp Stem Cell
MSC	Mesenchymal Stem Cell
PBS	Phosphate Buffer Saline
PCR	Polymerase Chain Reaction
PDMS	Polydimethylsiloxane
NGF	Nerve Growth Factor
NT-3	Neurotrophin-3
TGG	Trigeminal Ganglia

ABSTRACT

Mesenchymal stem cells (MSCs) have the capacity to self-renew and differentiate into specific cell types and are therefore key players during tissue repair and regeneration. The use of MSCs for the regeneration of tissues in vivo is increasingly being explored and already constitutes a promising alternative to existing clinical treatments. MSCs also exert paracrine and trophic functions, including the promotion of innervation that plays fundamental roles in regeneration and in restoration of the function of organs. Human bone marrow stem cells (hBMSCs) and human dental pulp stem cells (hDPSCs) have been used in studies aimed at the repair and/or regeneration of bone or other tissues of the craniofacial complex. However, the capabilities of hBMSCs and hDPSCs to elicit the growth of specific axons in order to re-establish functional innervation of the healing tissues are not known. Here we compared the neurotrophic effects of hDPSCs and hBMSCs on trigeminal and dorsal root ganglia neurons using microfluidic organs-on-chips devices. We found that hDPSCs express significantly higher levels of neurotrophins than hBMSCs and consequently neurons co-cultured with hDPSCs develop longer axons in the microfluidic co-culture system when compared to neurons co-cultured with hBMSCs. Moreover, hDPSCs elicited the formation of extensive axonal networks and established close contacts with neurons, a phenomenon not observed in presence of hBMSCs. Taken together these findings indicate that hDPSCs constitute a superior option for restoring the functionality of damaged craniofacial tissues, as they are able to support and promote extensive trigeminal innervation.

INTRODUCTION

Mesenchymal stem cells (MSCs) have attracted significant attention in last decades because of their potential use in regenerative medicine. MSCs are characterized by the ability to differentiate along the osteogenic, chondrogenic and adipogenic lineages, and can thus be exploited in therapeutic regimens aimed at the regeneration of different tissues such as bone and cartilage. Apart from their differentiation potential, MSCs have been shown to exert paracrine and trophic effects, including immunomodulation, augmentation of angiogenesis and neurogenesis, and promotion of cell survival [1].

MSCs have been isolated from many organs, and although all these different cell populations display similar differentiation potential, they vary in their trophic properties [2–5]. Human bone marrow stem cells (hBMSCs) represent the golden standard for bone repair, and have been used in studies aiming to regenerate various osseous structures, including craniofacial bones [6]. Dental MSCs were initially isolated from the pulp of human third molars [7] and since then dental MSCs have also been isolated from other locations, such as the pulp of exfoliated deciduous teeth, the apical papilla, the dental follicle, and the periodontal ligament [8]. These dental-derived MSCs populations vary in their expression of stem cell surface markers and in their ability to differentiate into distinctive cell lineages [9].

Human dental pulp stem cells (hDPSCs) have been extensively studied and in a dental clinical setting constitute very attractive candidates for cell-based regenerative therapies [10–12]. *In vitro* *h*DPSCs display a pattern of protein expression similar to hBMSCs [5]. However compared to hBMSCs, hDPSCs exhibit higher clonogenic and proliferative potentials, and they maintain a high rate of proliferation even after extensive sub-culturing [5]. hDPSCs originate from craniofacial embryonic tissues that do not express the Hox genes and therefore are not affected by the Hox-code as are other body tissues from where hBMSCs are derived [13]. Hox-genes are expressed in a spatially distinct pattern along the body axis where they provide cells with positional information [14, 15]. The absence of *Hox* genes in DPSCs confers them with a peculiar plasticity, as demonstrated by their ability to fully embrace the Hox-code of the site of engraftment upon transplantation in ectopic compartments [16]. In contrast, BMSCs transplanted into the craniofacial complex maintain the Hox-code of the tissue of origin, which hinders their differentiation [16]. Therefore, DPSCs are deemed preferable candidates for the regeneration of teeth and other craniofacial tissues [11, 17, 18].

A key component for successful repair processes is the efficient re-establishment of the appropriate neuronal network within the regenerating tissue. Indeed, innervation plays fundamental roles in the formation, homeostasis, and function of most tissues and organs [19]. Different classes

of nerve fibers exert distinctive functions in the various organs [19–21]. Sensory neurons projecting from the trigeminal ganglion provide sensation to most craniofacial tissues and organs [22]. In teeth, myelinated and non-myelinated trigeminal neurons convey sensory information [19, 23]. Craniofacial pathologies, traumas and interventions are commonly associated with impairment or loss of trigeminal innervation, which can result in long term neurosensory and functional disturbances [22, 24]. In severe cases, nerves resected from other parts of the body are grafted to achieve trigeminal nerve repair, but this is a highly invasive procedure with suboptimal outcomes [25]. Recent scientific evidence supports the notion that nerve-derived signals also play an important role in the repair of orofacial tissues. For example, in salivary glands, parasympathetic neurons secrete signals that are necessary for the activation of stem/progenitor cells during regenerative processes [26, 27]. It is becoming clear that in stem cell-based therapies it is essential to promote accurate re-innervation of regenerating tissues and elicit the growth of axons from specific neuronal subtypes. Therapies aiming at craniofacial regeneration thus need to re-establish proper trigeminal innervation to ensure an effective tissue repair and functionality.

The study of cell-cell interactions is increasingly supported by state-of-the-art culture and co-culture systems. Among these, organs-on-chips represent the most promising tools to emulate and study *in vivo* complex microenvironments. Organs-on-chips are devices with separate compartments lined by living cells and provide effective *in vitro* tools for recapitulating and mimicking multicellular architecture, cell-cell interactions, and physical microenvironment of functional units of living organs [28]. These models allow precise control of the secreted signaling molecules and provide a real time readout on basal cell functions that permits the reconstitution of organ physiology.

Here we investigated the neurotrophic effects of hDPSCs and hBMSCs on trigeminal and dorsal root ganglia using a microfluidic organ-on-chip system. The results showed that, compared to hBMSCs, hDPSCs express higher levels of neurotrophins, promote longer axon growth and formation of extensive neuronal networks, and establish numerous and tight connections with nerve fibers.

MATERIALS AND METHODS

Collection of human cells

The procedure for anonymized human dental pulp stem cells (hDPSCs) collection at the Zentrum für Zahnmedizin, Zürich, was approved by the Kantonale Ethikkommission of Zurich (reference number 2012-0588) and the patients gave their written informed consent. All procedures were performed in accordance with the current guidelines. Tooth extractions were performed by professional dentists. Human bone marrow stromal/stem cells (hBMSCs) were kindly provided by Prof. Ivan Martin (University Hospital Basel, Basel, Switzerland) and Prof. Franz Weber (University of Zurich, Zurich, Switzerland; cells from ATCC).

Cell culture and expansion

hDPSCs were expanded as monolayers on T-150 culture flasks (Sarsted AG, Switzerland) in Dulbecco's Modified Eagle Medium: Nutrient Mixture F-12 (DMEM/F12; ThermoFisher / Life Technologies, Switzerland) supplemented with 10% Fetal Bovine Serum (FBS, Bioswisstech AG, Switzerland), 100 U/ml penicillin/streptomycin (Sigma-Aldrich/Merck, Darmstadt, Germany), and Amphotericin B 0.25 µg/µL (ThermoFisher Scientific, Switzerland) incubated at 37°C in 5% CO2. hBMSCs were expanded in MesenPro medium (Cat. n°: 12746012, ThermoFisher). The medium was replaced every second day. Cells were passaged once a confluence of 70-80% was reached. Cells were washed once with phosphate buffered saline (PBS) before trypsin was added for 3 min at 37°C for their detachment. Trypsin was blocked by addition of 5 volumes of DMEM/F12 supplemented with 10% FBS.

Gene expression analysis - Real time PCR

Cells were collected by trypsinization, snap-frozen in liquid nitrogen and stored at -80°C. Trigeminal ganglia (TGG) and dorsal root ganglia (DRG) were dissected, immediately snap-frozen in liquid nitrogen and stored at -80°C.

RNA isolation and purification. RNA isolation on snap-frozen cells and TGG/DRG was performed with the RNeasy Plus Universal Mini Kit according to the instructions (Qiagen AG, Hombrechtikon ZH, Switzerland).

cDNA synthesis. Reverse transcription of the isolated RNA was performed using the iScript™ cDNA synthesis Kit and according to the instructions given (Bio-Rad Laboratories AG, Cressier FR, Switzerland). Briefly, 1000 ng of RNA were used for reverse transcription into cDNA. Nuclease-free water was added to add up to a total of 15 µl. 4 µl of 5x iScript reaction mix and 1 µl of iScript reverse transcriptase were added per sample in order to obtain a total volume of 20 µl.

The reaction mix was then incubated for 5 min at 25°C, for 30 min at 42°C and for 5 min at 85°C using a Biometra TPersonal Thermocycler (Biometra AG, Göttingen, Germany).

Quantitative real-time PCR. The 3-step quantitative real-time PCRs were performed using an Eco Real-Time PCR System (Illumina Inc., San Diego CA, USA). Expression level analysis of *hGAPDH*, *m36B4* (housekeeping gene), h*NGF*, h*BDNF*, h*GDNF*, h*NT-3, mNtrk1*, *mNtrk2*, *mNtrk3*, *mNGFR* were carried out using the SYBR® Green PCR Master Mix (Applied Biosystems, Carlsbad CA, USA) in combination with specific oligonucleotide primers: *hNGF*, Fw: 5'- GGC AGA CCC GCA ACA TTA CT-3', Rv: 5'- CAC CAC CGA CCT CGA AGT C-3'; *hBDNF*, Fw: 5'- GGC TTG ACA TCA TTG GCT GAC-3', Rv: 5'- CAT TGG GCC GAA CTT TCT GGT-3'; *hGDNF*, Fw: 5'- AGC AGT GAC TCA AAT ATG CCA GA-3', Rv: 5'- GCC TCT CCG ACC TTT TCC TC-3'; *hNT-3*, Fw, 5'- AAC GCG ATG TAA GGA AGC CA-3', Rv: 5'- AGT GCT CGG ACG TAG GTT TG-3'; h*GAPDH*, Fw: 5'- AGG GCT GCT TTT AAC TCT GGT-3', Rv: 5'- CCC CAC TTG ATT TTG GAG GGA-3; mNtrk1, Fw: 5'-AGT TAC CTG GAC GTT CTG GG-3', Rv: 5'-TGC TGA GGG TGA GAG ACT TG-3'; mNtrk2, Fw: 5'- TGT GGC TCA AGA CTC TCC AG-3', Rv: 5'- AGA CTT TCC TTC CTC CAC GG-3'; mNtrk3, Fw: 5'- CTT TGA GTC TGA TGC GAG CC-3', Rv: 5'- TGG TGT AGT GAT GCC ATG GT-3'; mNGFR, Fw: 5'- CTG CCT TCC TCT GTC TGT CA-3', Rv: 5'- TTG GAT TAT GGG GTG GGT CC-3'.

The reaction mix was composed of 5 µl of SYBR® Green PCR Master Mix reverse and forward primers (200 nM), and 2 ng of template cDNA. The thermocycling conditions were: 95°C for 10 min, followed by 40 cycles of 95°C for 15 sec, 55°C for 30 sec and 60°C for 1 min. Melt curve analysis was performed at 95°C for 15 sec, 55°C for 15 sec and 95°C for 15 sec. Expression levels were calculated by the comparative ΔCt method ($2^{-\Delta Ct}$ formula), normalizing to the Ct-value of the GAPDH housekeeping gene. Gene expression analysis was performed on hDPSCs and hBMSCs isolated from 12 patients (hDPSCs and hBMSCs were derived from different patients).

ELISA assay

hDPSCs and hBMSCs were seeded in equal amounts in 10cm Petri dishes. Cells were cultured in Dulbecco's Modified Eagle Medium: Nutrient Mixture F-12 (DMEM/F12; ThermoFisher / Life Technologies, Switzerland) supplemented with 10% Fetal Bovine Serum (FBS, Bioswisstech AG, Switzerland), 100 U/ml penicillin/streptomycin (Sigma-Aldrich/Merck, Darmstadt, Germany) for 48 hours. The culture medium was collected and centrifuged at 1500 rpm for 10 minutes. The supernatant was further filtered with a 0.22 µm filter. Culture media were then analysed with ELISA kits against human NGF (EHNGF, ThermoFisher Scientific, Zurich, Switzerland), human BDNF (ab99978, Abcam, Cambridge, UK), human GDNF (EHGDNF,

ThermoFisher Scientific, Zurich, Switzerland), human Neutrophin-3 (NT3) (EHNT3, ThermoFisher Scientific, Zurich, Switzerland).

Western blot

Total protein extracts were prepared according to standard protocols from snap-frozen TGGs and DRGs. Proteins were subjected to SDS–polyacrylamide gel electrophoresis (SDS-PAGE) separation and blotting. The following antibodies were used: rabbit pAb anti-TrkA (1:100, Sigma-Aldrich, 06-574), rabbit pAb anti-TrkB (1:100, R&D Systems, AF1494), rabbit pAb anti-TrkC (1:100, R&D Systems, AF1404), rabbit mAb anti-nerve growth factor receptor (NGFR/p75) (1:100, Sigma-Aldrich, N3908). Antibody binding was detected by using an appropriate horseradish peroxidase–conjugated IgG and revealed by ECL (Lumi-Light Western Blotting Substrate, 12015200001, Merck, Darmstadt, Germany).

Preparation of microfluidic devices

Microfluidic devices were prepared as previously described [29, 30]. Glass coverslips were coated overnight at 37 °C with 0.1 mg/ml poly-D-lysine and stored in 70% ethanol at 4°C. Polydimethylsiloxane (PDMS) microfluidic devices (Millipore A150, Switzerland, 2x2cm) were punched with a 1mm - diameter biopsy punch on the neuronal side to enable the insertion of the trigeminal ganglion and then sterilized with 70% ethanol. Both glass coverslips and microfluidic devices were then let dry completely under the laminar flow hood for approx. 2 hours. In sterile conditions, glass coverslips were placed in a 6-wells plate. The microfluidic devices were then mounted onto the glass coverslips and pressed gently to ensure proper adhesion. After mounting, the microfluidic devices were coated with laminin (5µg/ml, in Neurobasal medium) overnight at 37 °C. In order to prevent the persistence of air bubbles in the culture chambers, the coated microfluidic devices were placed under vacuum. After coating, the laminin solution was removed, and the culture chambers filled with the appropriate culture medium.

Mouse handling and trigeminal and dorsal root ganglia dissection

All mice were maintained and handled according to the Swiss Animal Welfare Law and in compliance with the regulations of the Cantonal Veterinary Office, Zurich (License number: 151/2014). C57/BL6J mice were time-mated. Successful mating was assessed by vaginal plug check, and day of plug was considered as day of embryonic development 0.5 (E0.5). Trigeminal ganglia and dorsal root ganglia were dissected from embryonic day 14.5-16.5 (E14.5-E16.5) mouse embryos. Dissections were performed in cold Dulbecco's phosphate buffered saline (PBS). Dissected ganglia were preserved in PBS, on ice, until culture**.**

Trigeminal ganglia and dorsal root ganglia were then cultured in Neurobasal medium (Gibco) supplemented with B27 (Gibco 17504-044), GlutaMAX, penicillin/streptomycin (10U/ml), 50 ng/ml nerve growth factor (NGF, R&D Systems) and 0.25 pM Arabinose Cytoside.

Co-culture of trigeminal and dorsal root ganglia and hMSCs

Trigeminal ganglia and dorsal root ganglia were placed through the punched hole into the neuronal chamber of the microfluidic device [29]. Ganglia were cultured alone for 5-7 days, until axons were projected into the stem cells chamber. Cells were then added to the co-culture system. 20 µl of hDPSCs or hBMSCs were added directly in the stem cell chambers at a density of $1*10^4$ cells/chamber. Cells were let attach for 1 hour and 30 minutes; then 300 µl of the appropriate medium were added to all chambers. Co-cultures were maintained for four days. At the end of the culture period, medium was removed, and all chambers were washed once with 300 µl PBS for 10 minutes. Afterwards, the samples were fixed in paraformaldehyde 4% (PFA 4%), 300 µl/ chamber, for 15 minutes. Chambers were then washed again with 300 µl PBS/chamber for 10 minutes and were stored at 4°C in PBS.

Immunofluorescent staining

Fixed samples were permeabilised by incubating them in 1% Triton/PBS for ten minutes. Non-specific sites were blocked with PBS, 0.1% Triton and 1% bovine serum albumin (BSA) for 30 minutes at RT, 90-100µl per chamber. Trigeminal ganglia, dorsal root ganglia and co-cultures were incubated overnight with the following primary antibodies (1° AB): mouse IgG1 α-neurofilament (α-NF) antibody (1:100, Hybridoma Bank, Iowa City, USA), rabbit mAb anti-neurofilament (1:200, Cell Signaling Technology, 2837), rabbit pAb anti-Peripherin (1:200, Abcam, ab4666), mouse mAb anti-Vimentin (1:100, DAKO, M0725), rabbit mAb anti-TrkA (1:50, Abcam, ab76291), rabbit pAb anti-TrkA (1:100, Sigma-Aldrich, 06-574), rabbit pAb anti-TrkB (1:100, R&D Systems, AF1494), rabbit pAb anti-TrkC (1:100, R&D Systems, AF1404), rabbit mAb anti-nerve growth factor receptor (NGFR/p75) (1:100, Sigma-Aldrich, N3908), mouse mAb anti- Calcitonin Gene Related Peptide (CGRP) (1:200, Abcam, ab81887), rabbit pAb anti-β-III-tubulin (1:200, Abcam, ab18207), rabbit pAb anti-Synapsin I (1:100, Abcam, ab64581), rabbit pAb anti-human-Nuclear Mitotic Antigen (NuMA, 1:100, GeneTex, GTX113510) diluted in PBS supplemented with 1% bovine serum albumin (BSA). The samples were washed three times (5 minutes each) with PBS + 0.5% Tween. The co-cultures were then incubated overnight with the following secondary antibodies (50-60µl per chamber): Alexa-Fluor488 conjugated anti-Rabbit (A-11034, ThermoFisher), Alexa-fluor568 conjugated anti-mouse (A-11004, ThermoFisher) diluted 1:250 in 1% BSA/PBS. Co-cultures were then washed three times (5 minutes each) with PBS and successively incubated with

4',6-diamidino-2-phenylindole (DAPI) for ten minutes at RT. Samples were finally washed twice (5 minutes each) with PBS. Microfluidic devices were then removed from the 6-wells plates and mounted on slides. TGG and DRG were cleared with Focus Clear (CelExplorer) overnight at 4°C. Co-cultures were imaged with a Leica DM6000 microscope equipped with a Leica DFC350FX camera and the Leica Application Suite Advanced Fluorescence (LAS AF) software. TGGs and DRGs were imaged with a Leica SP8 Confocal Laser Scanning Microscope (CLSM). Tile scans were stitched using the Mosaic J plugin of Fiji/Imagej [31] and manually aligned when needed.

The same protocol was applied for the immunofluorescent imaging of neurotrophins in hDPSCs and hBMSCs. The following primary antibodies were used: Goat pAb anti-human β-nerve growth factor (NGF) (1:100, R&D Systems, AF-256-NA), mouse mAb anti-brain derived neurotrophic factor (BDNF) (1:100, R&D Systems, MAB248-100), rabbit pAb anti-glia derived neurotrophic factor (GDNF) (1:100, Abcam, ab18956), rabbit pAb anti-neutrophin 3 (NT-3) (1:100, Abcam, ab65804). The following secondary antibodies were used: Alexa-568-conjugated anti-Rabbit (A-11011, ThermoFisher), anti-Goat (A11057, ThermoFisher), anti-Mouse (A-11004, ThermoFisher). Cells were then counterstained with phalloidin (A12379, ThermoFisher) and DAPI, and mounted with ProLong Diamond Antifade mounting medium (P36965, ThermoFisher). Staining was imaged with a Leica SP8 Confocal Scanning Laser Microscope.

Quantification of axonal growth

Axonal growth was quantified using AxoFluidic (developed by Estrela Neto [32]). AxoFluidic© uses the following function to model and quantify axonal growth:

$(x)=A\ x\exp(-\ x\lambda)$, with: A: degree of axons that effectively cross the grooves; X: spatial variable; λ: scale of spatial decay → length of neurites.

Analysis was performed on n = 4 microfluidic co-cultures per condition, and A and λ values plotted and analyzed with GraphPad Prism 8.0©.

RESULTS

Human dental pulp stem cells and human bone marrow stromal cells express neurotrophins

We first investigated whether hDPSCs and hBMSCs express neurotrophins (NTFs), key promoters of axonal outgrowth. We thus analyzed by real time PCR the expression of the genes coding for nerve growth factor (*NGF*), brain-derived neurotrophic factor (*BDNF*), glial-derived neurotrophic factor (*GDNF*) and neurotrophin-3 (*NT-3*). Expression of all genes was detectable in both hDPSCs and hBMSC. We observed that, compared to hBMSCs, hDPSCs express higher levels of all these NTFs. The highest difference was observed in the expression of *GDNF* and *NT-3*, with hDPSCs expressing 5-10-fold higher levels of these genes (Fig. 1C, D). *NGF* expression was also higher in hDPSCs (Fig. 1A). In contrast, *BDNF* expression did not differ significantly between the two cell populations (Fig 1B).

We verified the expression of NTFs at the protein level. Immunofluorescent staining showed expression of NGF, BDNF, GDNF and NT-3 both in hDPSCs (Figure 1E-H) and hBMSCs (Figure 1I-L; Figure 1M: negative control). NGF, BDNF and GDNF were also secreted in the culture medium at low, but detectable levels (Figure 1N-P). These three neurotrophic factors were found in higher concentrations in the medium exposed to hDPSCs (Figure 1N-P).

Co-culture of trigeminal or dorsal root ganglia and MSCs in microfluidic devices

We then set out to investigate whether hDPSCs and hBMSCs exert different neurotrophic effects on trigeminal and dorsal root neurons.

We first optimized the conditions for the culture of whole trigeminal ganglia, dorsal root ganglia, and hDPSCs or hBMSCs. Ganglia were isolated from E14.5-E16.5 C57/BL6J mouse embryos and cultured alone on the somal side for 4 days. Neurotrophin receptors TrkA, TrkB, TrkC and p75/NGFR could be detected in both trigeminal and dorsal root ganglia both at the mRNA and protein level, (Figure 2A-H; J-L). Similar to what is observed *in vivo* [33–35], trigeminal and dorsal root ganglia expressed the sensory neuron marker CGRP (Calcitonin Gene Related Peptide; Figure 2I).

We then compared the neurotrophic properties of hDPSCs and hBMSCs. For our study we exploited an Organs-on-Chips system composed of a PDMS (Polydimethylsiloxane) microfluidic device mounted on a poly-D-lysine- and laminin-coated glass coverslip (Figure 3A, 3E). The device is a two-chamber system, each composed of two wells and an interconnected channel, separated by a set of 150 µm long, 5 µm wide microgrooves. The hydrostatic pressure formed by the volume differential between chambers induces fluidic isolation of the solution on the low volume side of the

device. Medium exchange was additionally limited by changing the culture medium every 48 hours. This system allows the culture of neuronal cell bodies and mesenchymal stem cells in their own culture media. As trigeminal neurons cell bodies and mesenchymal stem cells have different culture media requirements [30], this set up is optimal for the correct emulation of physiological interactions between these cell types. For culture of whole trigeminal ganglia, a hole of 1mm of diameter was performed with a biopsy punch in the middle of a culture chamber 1 (Figure 3B, F). Axonal outgrowth is limited to narrow and parallel channels, and the resultant behavior can be easily imaged. This system is thus a powerful tool for the study of neurites and synaptic formation.

We thus exploited this system to compare the neurotrophic properties of hDPSCs and hBMSCs. To this end, we analyzed neurite outgrowth of trigeminal ganglia co-cultured with hDPSCs and hBMSCs. Once trigeminal axonal outgrowth was detected on the axonal side, target cells were added to the microfluidic device (Figure 3A, B, E, F). Trigeminal ganglia and target cells were co-cultured for 4 days, stained for the pan-neuronal marker neurofilament and then analyzed by wide-field fluorescent microscopy (Figure 3C, D, G, H). We observed that trigeminal ganglia formed nerve-like structures, with large axon bundles forming both on the somal and the axonal side (Figure 3D). Most axons projecting from trigeminal ganglia and neurons cultured with hDPSCs reached the most distant end of the axonal chamber (Figure 3D). In contrast, most axons grown in presence of hBMSCs did not reach the opposite end of the axonal chamber within the culture period (Figure 3H). Axonal outgrowth was quantified using the Axofluidic software [32]. The analysis showed that trigeminal ganglia when co-cultured with hDPSCs grew significantly longer axons than when co-cultured with hBMSCs (Fig. 3I, λ-value). At the same time, no difference was detected in the fraction of axons that reached the axonal side upon culture with hDPSCs or hBMSCs (Fig. 3I, A constant).

We next performed an analogous experiment by co-culturing hDPSCs or hBMSCs with dorsal root ganglia (DRG) (Figure 4A-F). DRG innervate non-cranial bones, and hBMSCs, *in vivo* [36], while they do not target hDPSCs. Similar to what observed for TGG, hDPSCs promoted the growth of longer axons (Figure 4G), while not influencing the proportion of axons that reach the axonal chamber (Figure 4H).

Axonal branching and establishment of axon-cells contacts

We further analyzed the pattern of axonal growth and the establishment of axon/target contacts in presence of hDPSCs or hBMSCs. Staining against the neuronal markers βIII-tubulin and neurofilament, and the MSCs marker vimentin showed that hDPSCs elicit the formation of complex axonal networks, which establish extensive and recurrent contacts with target cells (Fig. 5A, C). To

investigate whether these contacts are associated with synapses, we performed immunostaining against Synapsin I, a neuronal phosphoprotein that coats synaptic vesicles and modulates neurotransmitter release. We observed that the dense axonal networks contacting hDPSCs were characterized by very evident accumulation of Synapsin I (Figure 5C, D).

In contrast to what observed with hDPSC, axons innervating hBMSCs had a more linear course, with less abundant collateral branches and less extensive contacts with the target cells (Figure 5B, E). Accordingly, accumulation of Synapsin I was only detectable at the few sites of contact between trigeminal axons and hBMSCs (Figure 5E, F).

DISCUSSION

Continuous efforts are spent to identify easily accessible sources of MSCs that could be successfully applied in clinics, not only for their regenerative properties, but also for taking advantage of their modulatory effects on the surrounding tissues [1, 6, 37]. Although the final clinical success of tissue regeneration relies heavily on understanding the mode of action of MSCs, in many cases their clinical use has proceeded the necessary understanding of their physiology [37]. Only lately, attention has been drawn to the fact that MSCs isolated from different sources are not only developmentally different but also widely diverge in their transcriptomic signatures, differentiation potential and biological functions [37, 38]. Among these, the promotion of the innervation of the regenerated tissue is an often neglected but fundamental aspect. Correct innervation is necessary for the function of most organs, including bone [39, 40] and teeth [12, 19, 41]. Innervation modulates bone development and remodeling [39, 42], and it is directly involved in tooth reparative processes [43, 44]. Craniofacial traumatic injuries, as well as surgical interventions, often lead to trigeminal nerve damage or resection, resulting not only in the loss of sensation but also in the impairment of homeostatic and regenerative processes that depend on nerve-derived signals [22, 24, 45, 46]. Any regenerative therapy should thus also integrate the innervation of the repaired tissue. Nerve fibers should not be only attracted towards their targets, i.e. the regenerating tissues, but they should also form long-lasting functional contacts and interactions.

Our results clearly show that, compared to hBMSCs, hDPSCs elicit the growth of longer axons, both from trigeminal and dorsal root ganglia neurons. This is noteworthy given that hBMSCs are considered the golden standard for MSC-mediated bone regenerative processes [38, 41]. In addition, hDPSCs may induce the formation of more extensive axonal networks, thus suggesting that their use in clinics for reparative purposes will confer tissues with an abundant and rich innervation. This is supported by findings in other damaged organs, such as the spinal cord and

391 retina, showing that hDPSCs display greater neurotrophic capabilities than hBMSCs [47, 48]. This
392 is in agreement with our results showing that hDPSCs induce the growth of longer axons when co-
393 cultured with dorsal root ganglia, whose axons innervate non-cranial bones and hBMSCs *in vivo*
394 [36]. We and others showed that hDPSCs express and secrete higher levels of neurotrophins than
395 hBMSCs (Figure 2) [48], which could explain the superior neurotrophic effects of hDPSCs.
396 Nevertheless, the varied effects of different MSCs populations on afferent nerves depend on more
397 factors than the expression of neurotrophins [48]. Thus, hDPSCs might provide a plethora of
398 molecular cues beyond the expression and secretion of neutrophins that cumulatively result in the
399 observed higher axonal growth and extensive neuronal network. While numerous studies
400 investigated the neurotrophic properties of hDPSCs and hBMSCs in clinically relevant contexts
401 such as spinal cord injury [49, 50] and ischemia [51], surprisingly few studies focus on their effects
402 on trigeminal innervation. It has been long known that the responses of specific neuronal
403 populations to neurotrophic signals can significantly differ, partially due to the relative expression
404 of different neurotrophin receptors [52].
405 A pivotal challenge in craniofacial regeneration is the re-establishment of a correct and
406 functional trigeminal innervation, and thus the identification of a MSC population that can ensure
407 proper re-innervation specifically by trigeminal neurons is of paramount importance. Our study
408 provides evidence that for the regeneration of craniofacial tissues, which are innervated by
409 trigeminal nerves, hDPSCs represent a more suitable choice than hBMSCs. Sensory alterations and
410 damages to trigeminal nerves are common in maxillofacial surgical procedures involving both
411 tissue removal and regeneration, and constitute an important postoperative issue [24, 25, 46, 53,
412 54]. There is therefore a pressing need for proper therapeutic alternatives to ectopic nerve
413 engraftment, which is invasive and often suboptimal. As different studies have demonstrated the
414 potential of hDPSCs to regenerate craniofacial bone in human patients [55, 56], our results show
415 that these cells could also be the basis for the successful innervation of the regenerated tissue.
416 Increasing evidence indicates that “organs-on-chips” systems represent faithful models of *in*
417 *vivo* processes, and are now the method of choice for the emulation of complex *in vivo* processes in
418 controlled and defined environments [28, 57]. Human cells and tissues grown in these culture
419 devices can maintain higher levels of tissue-specific differentiated functions *in vitro* [58], and have
420 been used to model also pathological human conditions [59]. Thanks to these properties, organs-on-
421 chips are increasingly being used for the identification of new drugs and the study of their
422 pharmacokinetic and pharmacodynamic properties [58, 60]. As such, these systems could be
423 exploited to study the effects of neurotrophins, synthetic neurotrophin analogues [61] and other
424 therapeutic agents on the interactions between trigeminal neurons and their targets within the

craniofacial complex. Aside from the scientific advantages, the use of such systems for *in vitro* modelling is a key axis of the research aiming at the refinement, replacement and reduction (3R) of experimental animal use [62]. We already demonstrated that the co-culture system employed in this study can faithfully model the pattern of tooth innervation observed *in vivo* [30], strongly suggesting that the results observed in the current study are representative of *in vivo* conditions.

CONCLUSIONS

These results demonstrate that, compared to hBMSCs, hDPSCs induce more extensive axonal growth, the formation of a richer neuronal network, and allow establishment of connections between them and axons. This information is essential for the design of novel stem cell-based therapeutic approaches aimed at the appropriate re-innervation of damaged craniofacial tissues.

CONFLICTS OF INTEREST

The authors have no conflicts of interest to declare.

ACKNOWLEDGMENTS

This work was supported by funds from the University of Zurich (UZH). We thank the group of Prof. Franz Weber (UZH) for providing hBMSCs. We thank Miss Madeline Fellner (Institute of Oral Biology, UZH) for the technical support during the revision of the manuscript.

AUTHOR CONTRIBUTIONS

P.P: Conception and design, collection and assembly of data, data analysis and interpretation, manuscript writing, final approval of manuscript. S. M.: Collection and assembly of data, data analysis and interpretation, contribution to writing of Methods section, final approval of manuscript. E.N: Collection and assembly of data, data analysis and interpretation, final approval of manuscript. I. M.: Provision of study material, data analysis and interpretation, final approval of manuscript. M.L.: Data analysis and interpretation, final approval of manuscript. T.A.M.: Conception and design, financial support, administrative support, provision of study material, data analysis and interpretation, manuscript writing, final approval of manuscript.

REFERENCES

1. Fu Y, Both SK, Wu L, et al (2017) Trophic Effects of Mesenchymal Stem Cells in Tissue Regeneration. Tissue Eng Part B Rev 23:515–528. https://doi.org/10.1089/ten.teb.2016.0365
2. Abbas OL, Musmul A, Özatik O, et al (2018) Comparative Analysis of Mesenchymal Stem Cells from Bone Marrow, Adipose Tissue, and Dental Pulp as Sources of Cell Therapy for Zone of Stasis Burns. J Investig Surg 1939:1–14. https://doi.org/10.1080/08941939.2018.1433254
3. Ando K, Kimura A, Abe T, et al (2018) Comparative characterization of stem cells from human exfoliated deciduous teeth, dental pulp, and bone marrow–derived mesenchymal stem cells. Biochem Biophys Res Commun 501:193–198. https://doi.org/10.1016/j.bbrc.2018.04.213
4. Isobe Y, Koyama N, Nakao K, et al (2016) Comparison of human mesenchymal stem cells derived from bone marrow, synovial fluid, adult dental pulp, and exfoliated deciduous tooth pulp. Int J Oral Maxillofac Surg 45:124–131. https://doi.org/10.1016/j.ijom.2015.06.022
5. Tamaki Y, Nakahara T, Ishikawa H, Sato S (2013) In vitro analysis of mesenchymal stem cells derived from human teeth and bone marrow. Odontology 101:121–32. https://doi.org/10.1007/s10266-012-0075-0
6. Tollemar V, Collier ZJ, Mohammed MK, et al (2016) Stem cells, growth factors and scaffolds in craniofacial regenerative medicine. Genes Dis 3:56–71. https://doi.org/10.1016/j.gendis.2015.09.004
7. Gronthos S, Mankani M, Brahim J, et al (2000) Postnatal human dental pulp stem cells (DPSCs) in vitro and in vivo. Proc Natl Acad Sci U S A 97:13625–30. https://doi.org/10.1073/pnas.240309797
8. Huang GT-JT-J, Gronthos S, Shi S (2009) Mesenchymal stem cells derived from dental tissues vs. those from other sources: their biology and role in regenerative medicine. J Dent Res 88:792–806. https://doi.org/10.1177/0022034509340867
9. Mitsiadis TA, Orsini G, Jimenez-Rojo L (2015) Stem cell-based approaches in dentistry. Eur Cells Mater 30:248–257. https://doi.org/DOI: 10.22203/eCM.v030a17
10. Orsini G, Pagella P, Mitsiadis TA (2018) Modern Trends in Dental Medicine: An Update for Internists. Am J Med 131:1425–1430. https://doi.org/10.1016/j.amjmed.2018.05.042
11. Orsini G, Pagella P, Putignano A, Mitsiadis TA (2018) Novel biological and technological platforms for dental clinical use. Front Physiol 9:1–12. https://doi.org/10.3389/fphys.2018.01102
12. Miran S, Mitsiadis TA, Pagella P (2016) Innovative Dental Stem Cell-Based Research Approaches: The Future of Dentistry. Stem Cells Int 2016:7231038. https://doi.org/10.1155/2016/7231038
13. Picchi J, Trombi L, Spugnesi L, et al (2013) HOX and TALE signatures specify human stromal stem cell populations from different sources. J Cell Physiol 228:879–889. https://doi.org/10.1002/jcp.24239
14. Pearson JC, Lemons D, McGinnis W (2005) Modulating Hox gene functions during animal body patterning. Nat Rev Genet 6:893–904. https://doi.org/10.1038/nrg1726
15. Mallo M, Wellik DM, Deschamps J (2010) Hox genes and regional patterning of the vertebrate body plan. Dev Biol 344:7–15. https://doi.org/10.1016/j.ydbio.2010.04.024
16. Leucht P, Kim J-B, Amasha R, et al (2008) Embryonic origin and Hox status determine progenitor cell fate during adult bone regeneration. Development 135:2845–54. https://doi.org/10.1242/dev.023788
17. La Noce M, Mele L, Tirino V, et al (2016) Neural crest stem cell population in craniomaxillofacial

development and tissue repair. Eur Cells Mater 28:348–357. https://doi.org/10.22203/ecm.v028a24
18. Alge DL, Zhou D, Adams LL, et al (2010) Donor-matched comparison of dental pulp stem cells and bone marrow derived mesenchymal stem cells in a rat model. J Tissue Eng Regen Med 4:73–81. https://doi.org/10.1002/term.220
19. Pagella P, Jiménez-Rojo L, Mitsiadis TA (2014) Roles of innervation in developing and regenerating orofacial tissues. Cell Mol Life Sci 71:2241–2251. https://doi.org/10.1007/s00018-013-1549-0
20. Kumar A, Brockes JP (2012) Nerve dependence in tissue, organ, and appendage regeneration. Trends Neurosci 35:691–9. https://doi.org/10.1016/j.tins.2012.08.003
21. Lucas D, Scheiermann C, Chow A, et al (2013) Chemotherapy-induced bone marrow nerve injury impairs hematopoietic regeneration. Nat Med 19:695–703. https://doi.org/10.1038/nm.3155
22. Gonella MC, Fischbein NJ, So YT (2009) Disorders of the trigeminal system. Semin Neurol 29:36–44. https://doi.org/10.1055/s-0028-1124021
23. Hildebrand C, Fried K, Tuisku F, Johansson CS (1995) Teeth and tooth nerves. Prog Neurobiol 45:165–222. https://doi.org/10.1016/0301-0082(94)00045-J
24. Sandstedt P, Sörensen S (1995) Neurosensory disturbances of the trigeminal nerve. A long-term follow-up of traumatic injuries. J Oral Maxillofac Surg 53:498–505. https://doi.org/10.1016/0278-2391(95)90055-1
25. Jones RHB (2010) Repair of the trigeminal nerve: A review. Aust Dent J 55:112–119. https://doi.org/10.1111/j.1834-7819.2010.01216.x
26. Knox SM, Lombaert IMA, Haddox CL, et al (2013) Parasympathetic stimulation improves epithelial organ regeneration. Nat Commun 4:1494. https://doi.org/10.1038/ncomms2493
27. Knox SM, Lombaert IM a, Reed X, et al (2010) Parasympathetic innervation maintains epithelial progenitor cells during salivary organogenesis. Science 329:1645–7. https://doi.org/10.1126/science.1192046
28. Ingber DE (2018) Developmentally inspired human 'organs on chips.' Development 145:dev156125. https://doi.org/10.1242/dev.156125
29. Pagella P, Miran S, Mitsiadis TA (2015) Analysis of developing tooth germ innervation using microfluidic co-culture devices. J Vis Exp. https://doi.org/10.3791/53114.
30. Pagella P, Neto E, Jiménez-Rojo L, et al (2014) Microfluidics co-culture systems for studying tooth innervation. Front Physiol 5 AUG: https://doi.org/10.3389/fphys.2014.00326
31. Schindelin J, Arganda-Carreras I, Frise E, et al (2012) Fiji: an open-source platform for biological-image analysis. Nat Methods 9:676–82. https://doi.org/10.1038/nmeth.2019
32. Neto E, Alves CJ, Sousa DM, et al (2014) Sensory neurons and osteoblasts: close partners in a microfluidic platform. Integr Biol (Camb) 6:586–95. https://doi.org/10.1039/c4ib00035h
33. Ichikawa H, Matsuo S, Sugimoto T (2012) Development of primary sensory neurons in the trigeminal nervous system; dependency on neurotrophins and other substances. Jpn Dent Sci Rev 48:48–52. https://doi.org/10.1016/j.jdsr.2011.10.001
34. Ichikawa H, Matsuo S, Silos-Santiago I, et al (2004) The development of myelinated nociceptors is dependent upon trks in the trigeminal ganglion. Acta Histochem 106:337–343. https://doi.org/10.1016/j.acthis.2004.07.003
35. Sullins JS, Carnes DL, Kaldestad RN, Wheeler EF (2000) Time course of the increase in trk A

expression in trigeminal neurons after tooth injury. J Endod 26:88–91. https://doi.org/S0099-2399(05)61007-2 [pii]\r10.1097/00004770-200002000-00007

36. Smith GM, Falone AE, Frank E (2012) Sensory axon regeneration: rebuilding functional connections in the spinal cord. Trends Neurosci 35:156–63. https://doi.org/10.1016/j.tins.2011.10.006

37. Martin I, Galipeau J, Kessler C, et al (2019) Challenges for mesenchymal stromal cell therapies. Sci Transl Med 11:eaat2189. https://doi.org/10.1126/scitranslmed.aat2189

38. Sacchetti B, Funari A, Remoli C, et al (2016) No identical “mesenchymal stem cells” at different times and sites: Human committed progenitors of distinct origin and differentiation potential are incorporated as adventitial cells in microvessels. Stem Cell Reports 6:897–913. https://doi.org/10.1016/j.stemcr.2016.05.011

39. Tomlinson RE, Li Z, Zhang Q, et al (2016) NGF-TrkA Signaling by Sensory Nerves Coordinates the Vascularization and Ossification of Developing Article NGF-TrkA Signaling by Sensory Nerves Coordinates the Vascularization and Ossification of Developing Endochondral Bone. Cell Rep 16:2723–2735. https://doi.org/10.1016/j.celrep.2016.08.002

40. Neto EC, Alves J, Ribas J, et al (2012) Disclosing the underlying interaction between bone and peripheral nervous system: Optimization of coculture systems. Bone 50:S113. https://doi.org/10.1016/j.bone.2012.02.347

41. Pagella P, Neto E, Lamghari M, Mitsiadis TA (2015) Investigation of orofacial stem cell niches and their innervation through microfluidic devices. Eur Cells Mater 29:213–223

42. Gkiatas I, Papadopoulos D, Pakos EE, et al (2017) The Multifactorial Role of Peripheral Nervous System in Bone Growth. Front Phys 5:1–6. https://doi.org/10.3389/fphy.2017.00044

43. Mitsiadis TA, Magloire H, Pagella P (2017) Nerve growth factor signalling in pathology and regeneration of human teeth. Sci Rep 7:1327. https://doi.org/10.1038/s41598-017-01455-3

44. Byers MR, Taylor PE (1993) Effect of Sensory Denervation on the Response of Rat Molar Pulp to Exposure Injury. J Dent Res 72:613–618. https://doi.org/10.1177/00220345930720031001

45. Stone JB, DeAngelis LM (2016) Cancer-treatment-induced neurotoxicity-focus on newer treatments. Nat Rev Clin Oncol 13:92–105. https://doi.org/10.1038/nrclinonc.2015.152

46. Susarla SM, Lam NP, Donoff RB, et al (2005) A comparison of patient satisfaction and objective assessment of neurosensory function after trigeminal nerve repair. J Oral Maxillofac Surg 63:1138–1144. https://doi.org/10.1016/j.joms.2005.04.021

47. Mead B, Logan A, Berry M, et al (2013) Intravitreally transplanted dental pulp stem cells promote neuroprotection and axon regeneration of retinal ganglion cells after optic nerve injury. Investig Ophthalmol Vis Sci 54:7544–7556. https://doi.org/10.1167/iovs.13-13045

48. Mead B, Logan A, Berry M, et al (2014) Paracrine-mediated neuroprotection and neuritogenesis of axotomised retinal ganglion cells by human dental pulp stem cells: Comparison with human bone marrow and adipose-derived mesenchymal stem cells. PLoS One 9:. https://doi.org/10.1371/journal.pone.0109305

49. Nosrat I V., Widenfalk J, Olson L, Nosrat CA (2001) Dental pulp cells produce neurotrophic factors, interact with trigeminal neurons in vitro, and rescue motoneurons after spinal cord injury. Dev Biol 238:120–32. https://doi.org/10.1006/dbio.2001.0400

50. Sakai K, Yamamoto A, Matsubara S, et al (2012) Human dental pulp-derived stem cells promote

locomotor recovery after complete transection of the rat spinal cord by multiple neuro-regenerative mechanisms. J Clin Invest 122:80–90. https://doi.org/10.1172/JCI59251.80

51. Lee J-H, Bu Y, Bae J, et al (2017) Human Dental Pulp Stem Cells are more Effective than Human Bone Marrow-Derived Mesenchymal Stem Cells in Cerebral Ischemic Injury. Cell Transplant 26:1001–1016. https://doi.org/10.3727/096368916x694391

52. Benedetti M, Levi a, Chao M V (1993) Differential expression of nerve growth factor receptors leads to altered binding affinity and neurotrophin responsiveness. Proc Natl Acad Sci U S A 90:7859–7863. https://doi.org/10.1073/pnas.90.16.7859

53. Elsalanty M, Genecov D (2009) Bone Grafts in Craniofacial Surgery. Craniomaxillofacial Trauma Reconstr 2:125–134. https://doi.org/10.1055/s-0029-1215875

54. Shibahara T, Noma H, Takasaki Y, Nomura T (2000) Repair of the inferior alveolar nerve with a forearm cutaneous nerve graft after ablative surgery of the mandible. J Oral Maxillofac Surg 58:714–717. https://doi.org/10.1053/joms.2000.7252

55. D'Aquino R, De Rosa A, Lanza V, et al (2009) Human mandible bone defect repair by the grafting of dental pulp stem/progenitor cells and collagen sponge biocomplexes. Eur Cells Mater 18:75–83

56. Giuliani A, Manescu A, Langer M, et al (2013) Three years after transplants in human mandibles, histological and in-line holotomography revealed that stem cells regenerated a compact rather than a spongy bone: biological and clinical implications. Stem Cells Transl Med 2:316–24. https://doi.org/10.5966/sctm.2012-0136

57. Leitão L, Lamghari M, Sousa DM, et al (2016) Compartmentalized Microfluidic Platforms: The Unrivaled Breakthrough of In Vitro Tools for Neurobiological Research . J Neurosci 36:11573–11584. https://doi.org/10.1523/jneurosci.1748-16.2016

58. Prantil-Baun R, Novak R, Das D, et al (2016) Physiologically-Based Pharmacokinetic and Pharmacodynamic Analysis Enabled by Microfluidically Linked Organs-on-Chips. Annu Rev Pharmacol Toxicol 58:37–64. https://doi.org/10.1146/annurev-pharmtox-010716-104748

59. Huh D, Leslie DC, Matthews BD, et al (2012) A human disease model of drug toxicity-induced pulmonary edema in a lung-on-a-chip microdevice. Sci Transl Med 4:159ra147. https://doi.org/10.1126/scitranslmed.3004249

60. Jain A, Barrile R, van der Meer ADD, et al (2018) Primary Human Lung Alveolus-on-a-chip Model of Intravascular Thrombosis for Assessment of Therapeutics. Clin Pharmacol Ther 103:332–340. https://doi.org/10.1002/cpt.742

61. Pediaditakis I, Kourgiantaki A, Prousis KC, et al (2016) BNN27, a 17-spiroepoxy steroid derivative, interacts with and activates p75 neurotrophin receptor, rescuing cerebellar granule neurons from apoptosis. Front Pharmacol 7:1–14. https://doi.org/10.3389/fphar.2016.00512

62. Sfriso R, Zhang S, Bichsel CA, et al (2018) 3D artificial round section micro-vessels to investigate endothelial cells under physiological flow conditions. Sci Rep 8:1–13. https://doi.org/10.1038/s41598-018-24273-7

Figure Legends

Figure 1. Expression of neurotrophins in hDPSCs and hBMSCs *in vitro*. A-D) Real time PCR analysis of the expression of genes coding for *NGF, BDNF, GDNF, NT3* in hDPSCs and hBMSCs isolated from different patients. Results are expressed in fold change to the expression level of *GAPDH*. **E-M)** Immunofluorescent staining showing the expression of NGF, BDNF, GDNF and NT-3 proteins (red color) in hDPSCs (E-H, upper row) and hBMSCs (I, L lower row). M: negative control. **N-P)** ELISA analysis of neurotrophins' secretion by cultured hDPSCs and hBMSCs. Abbreviations: NGF, nerve growth factor; BDNF, brain-derived neurotrophic factor; GDNF, glial-derived neurotrophic factor; NT-3, neurotrophin 3; GAPDH: Glyceraldehyde 3-phosphate dehydrogenase. Scale bars: 20 μm. * = $p < 0.05$; ** = $p < 0.01$.

Figure 2. Expression of neurotrophin receptors and neuronal-specific proteins in trigeminal and dorsal root ganglia. A) Bright-field image of a cultured trigeminal ganglion. **B-D)** Real time PCR analysis of the expression of genes coding for *Ntrk1*, *Ntrk2*, *Ntrk3*, *NGFR* in TGG and DRG. **E-K)** Immunofluorescent staining showing expression of TrkA, TrkB, TrkC, p75/NGFR, calcitonin gene related peptide (CGRP) and neurofilament in ganglia. **L)** Western blot confirming expression of TrkA, TrkB, TrkC and p75/NGFR in TGG. Scale bars: A, 2 mm; E-H: 500 μm; I-K: 40 μm.

Figure 3. Comparison of axonal growth from trigeminal ganglia (TGGs) co-cultured with hDPSCs or hBMSCs. A) Experimental approach for TGGs and hDPSCs co-culture. **B)** Brightfield overview of TGG co-cultured with hDPSCs **C)** Immunofluorescent staining (neurofilament, green color) showing exemplary axonal growth in presence of hDPSCs. **D)** Immunofluorescent staining showing growth of TGG axons (neurofilament, green color) in the presence of hDPSCs (DAPI, blue color). Notice that many axons reach the terminal end of the microfluidic chamber. White dotted lines show the borders of the microfluidic chamber containing hDPSCs. **E)** Experimental approach for TGGs and hDPSCs co-culture. **F)** Bright-field overview of TGG co-cultured with hBMSCs. **G)** Immunofluorescent staining (neurofilament, green color) showing exemplary axonal growth in presence of hBMSCs. **H)** Immunofluorescent staining showing growth of TGG axons (neurofilament, green color) in the presence of hBMSCs (DAPI, blue color). Notice that no or few axons reach the terminal end of the microfluidic chamber. White dotted lines show the borders of the microfluidic chamber containing hBMSCs. **I)** Graphs depicting the λ parameter, indicative of axonal length, and the A parameter, representing the fraction of axons that reach the axonal side.

649 Abbreviations: hBMSCs, human bone marrow stem cells; hDPSCs, human dental pulp stem cells;
650 mg, microgrooves; TGGs, trigeminal ganglia. Scale bars: B, F: 1 mm; D, H: 300 μm.

651 **Figure 4. Comparison of axonal growth from dorsal root ganglia (DRG) co-cultured with**
652 **hDPSCs or hBMSCs. A)** Overview of axonal growth from DRG cultured in the presence of
653 hDPSCs. **B, C)** Immunofluorescent staining showing contacts between axons (NF200, red color)
654 and hDPSCs (vimentin, green color). **D)** Overview of axonal growth from DRG cultured in the
655 presence of hBMSCs. **E, F)** Immunofluorescent staining showing contacts between axons (NF200,
656 red color) and hBMSCs (vimentin, green color). **G)** Graph depicting the λ parameter, indicative of
657 axonal length. **H)** Graph depicting the A parameter, representing the fraction of axons that reach the
658 axonal side. Abbreviations: hBMSCs, human bone marrow stem cells; hDPSCs, human dental pulp
659 stem cells; DRG, dorsal root ganglia. Scale bars: A, D: 300 μm; B, C, E, F: 50 μm.

660 **Figure 5. Trigeminal axons form extensive networks and contacts when cultured in the**
661 **presence of hDPSCs**. **A, B)** Immunofluorescent staining showing trigeminal axons networks (βIII-
662 tubulin, green color) innervating hDPSCs (A) and hBMSCs (B) (βIII-tubulin, green color; DAPI,
663 blue color). **C)** Immunofluorescent staining showing extensive contacts established by trigeminal
664 axons (neurofilament, green color) with hDPSCs (vimentin, red color). **D)** Immunofluorescent
665 staining showing strong accumulation of Synapsin (red color) at the contact sites between
666 trigeminal axons (neurofilament, green color) and hDPSCs (white dotted line: cell borders). **E)**
667 Immunofluorescent staining showing growth of trigeminal axons (neurofilament, green color)
668 mostly along and past hBMSCs (vimentin, red color). **F)** Immunofluorescent staining showing few
669 contacts (Synapsin accumulation, red color) established by trigeminal axons (neurofilament, green
670 color) with hBMSCs. White arrowheads: points of contact between trigeminal neurons and hDPSCs
671 or hDPSCs. Abbreviations: hBMSCs, human bone marrow stem cells; hDPSCs, human dental pulp
672 stem cells; TGG, trigeminal ganglion. Scale bars: A, B: 25 μm; C-F: 20 μm.

Figure 1

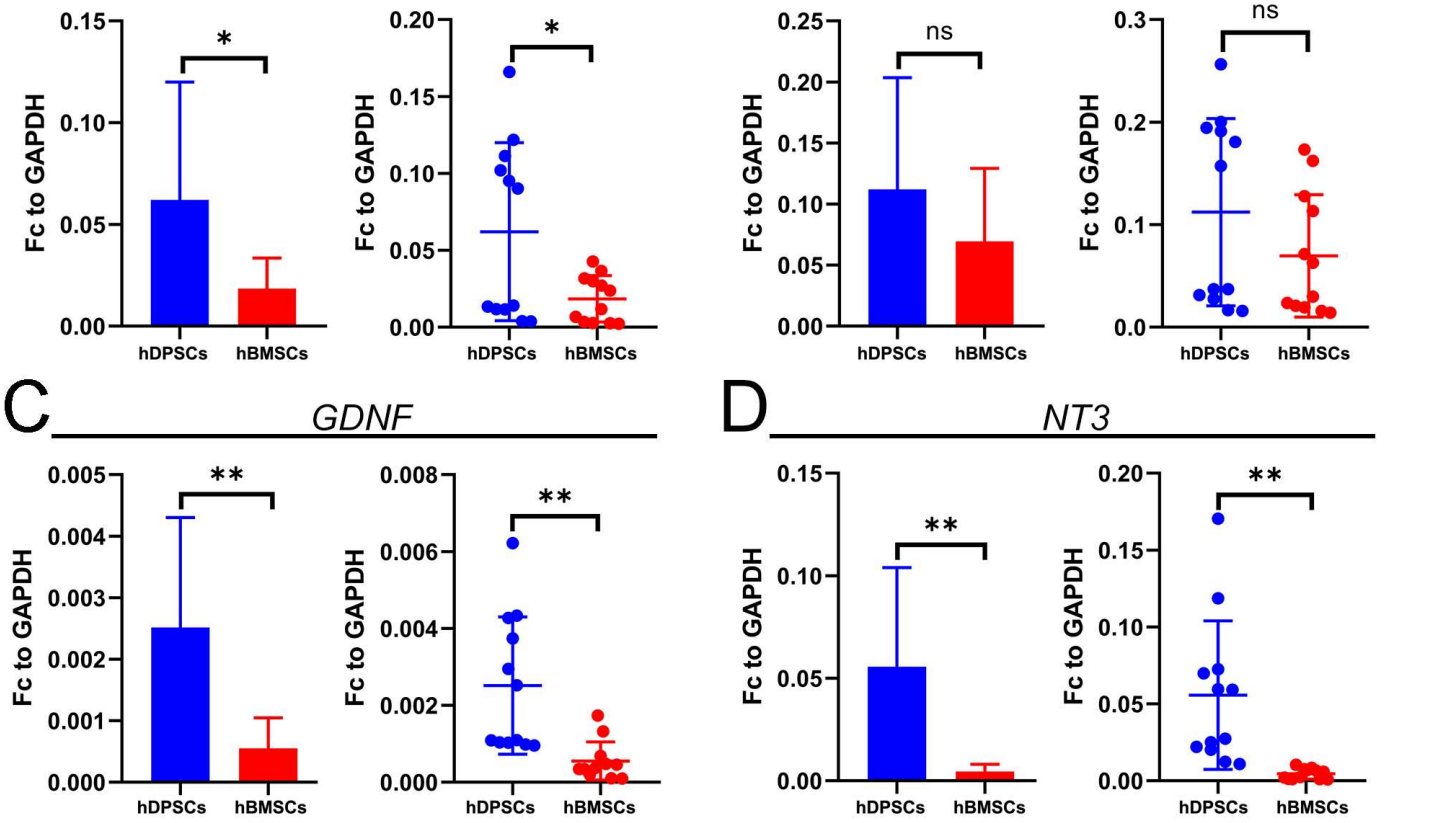
A
NGF
Fc to GAPDH
0.15
0.10
0.05
0.00
*
hDPSCs
hBMSCs
0.20
0.15
0.10
0.05
0.00
*
hDPSCs
hBMSCs
B
BDNF
Fc to GAPDH
0.25
0.20
0.15
0.10
0.05
0.00
ns
hDPSCs
hBMSCs
0.3
0.2
0.1
0.0
ns
hDPSCs
hBMSCs
C
GDNF
Fc to GAPDH
0.005
0.004
0.003
0.002
0.001
0.000
**
hDPSCs
hBMSCs
0.008
0.006
0.004
0.002
0.000
**
hDPSCs
hBMSCs
D
NT3
Fc to GAPDH
0.15
0.10
0.05
0.00
**
hDPSCs
hBMSCs
0.20
0.15
0.10
0.05
0.00
**
hDPSCs
hBMSCs

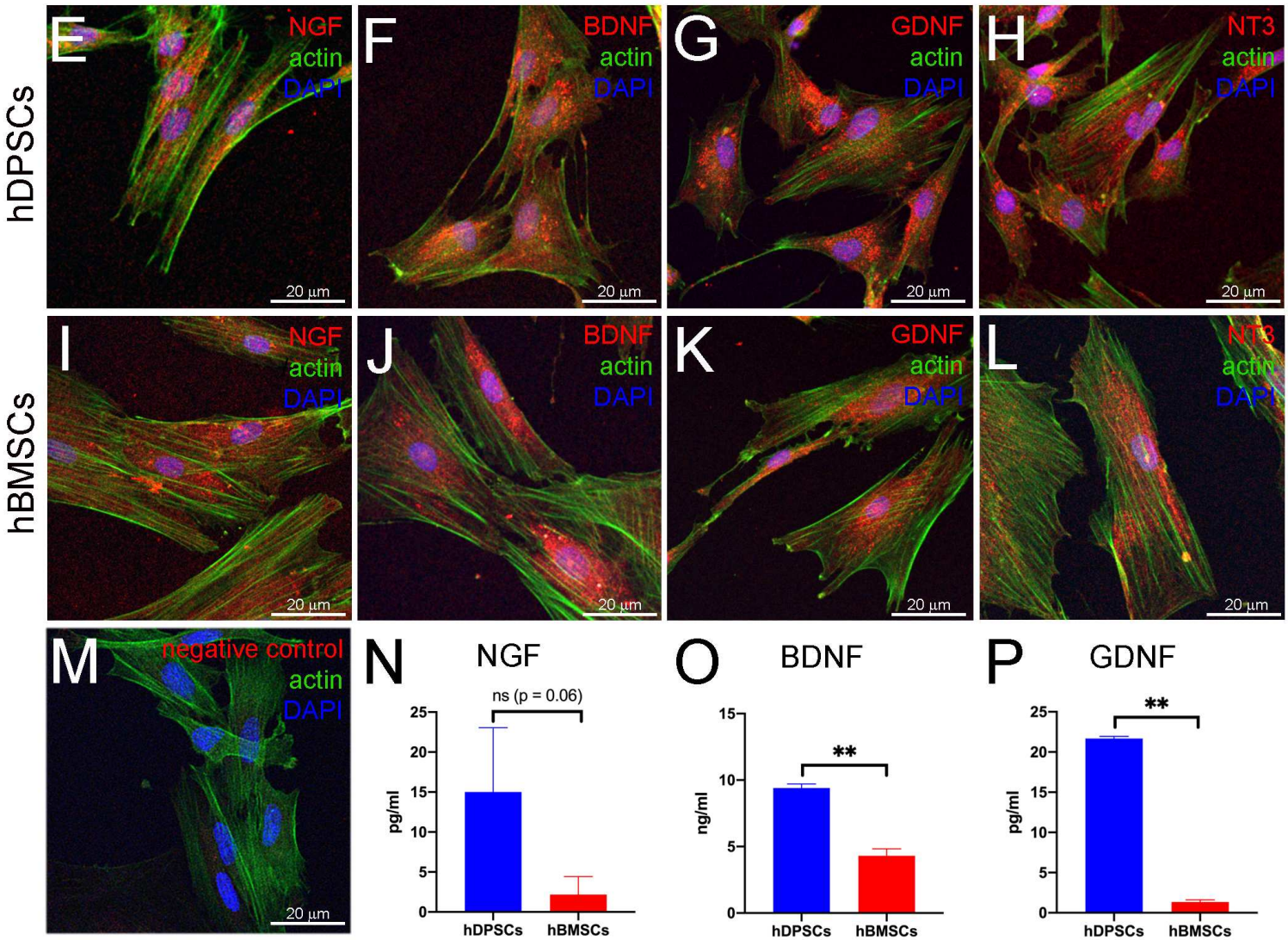
hDPSCs
hBMSCs
E
NGF
actin
DAPI
20 µm
F
BDNF
actin
DAPI
20 µm
G
GDNF
actin
DAPI
20 µm
H
NT3
actin
DAPI
20 µm
I
NGF
actin
DAPI
20 µm
J
BDNF
actin
DAPI
20 µm
K
GDNF
actin
DAPI
20 µm
L
NT3
actin
DAPI
20 µm
M
negative control
actin
DAPI
20 µm
N
NGF
ns (p = 0.06)
pg/ml
25
20
15
10
5
0
hDPSCs
hBMSCs
O
BDNF
ng/ml
15
10
5
0
**
hDPSCs
hBMSCs
P
GDNF
pg/ml
25
20
15
10
5
0
**
hDPSCs
hBMSCs

Figure 2

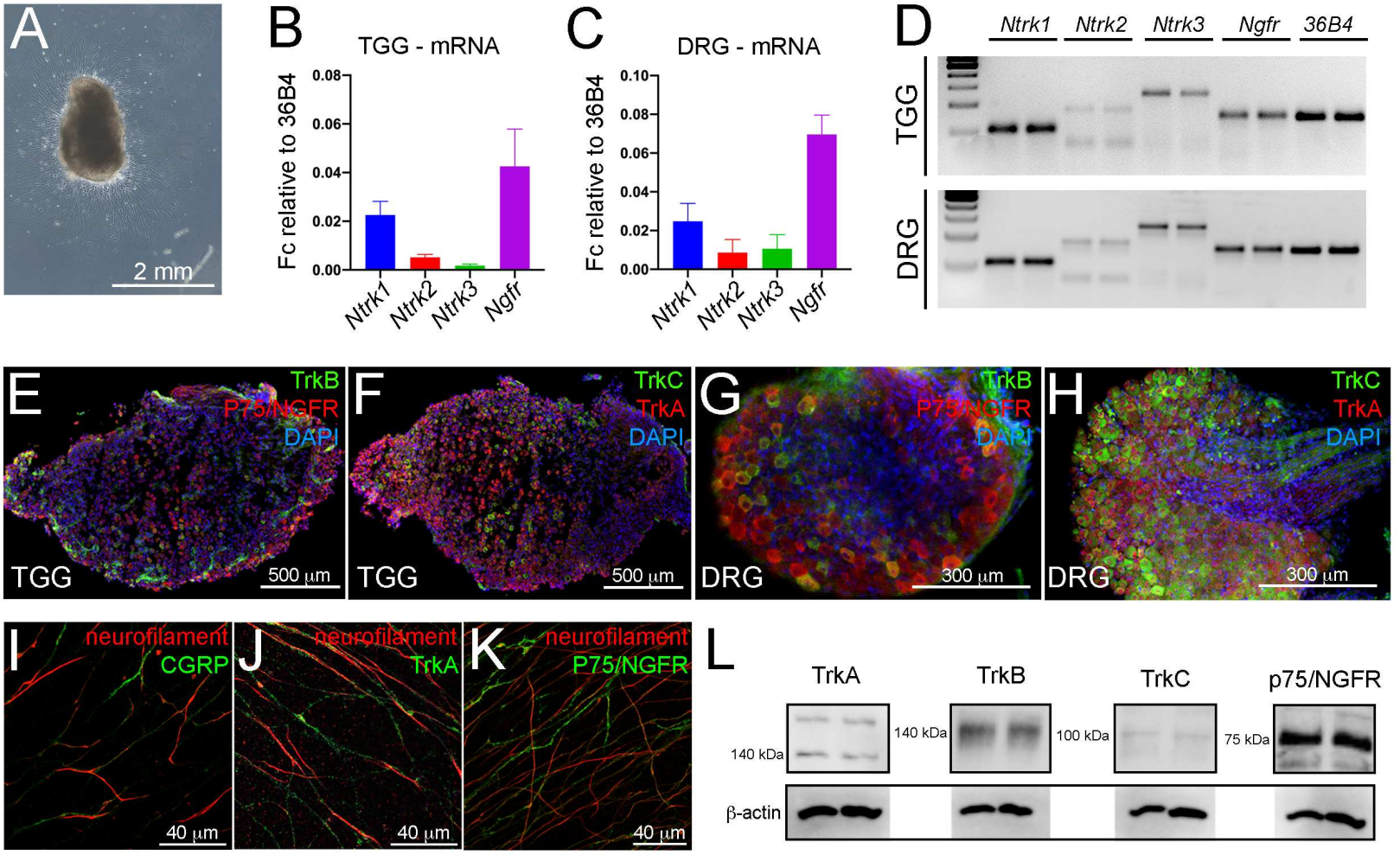
A
2 mm
B
TGG - mRNA
Fc relative to 36B4
0.08
0.06
0.04
0.02
0.00
Ntrk1
Ntrk2
Ntrk3
Ngfr
C
DRG - mRNA
Fc relative to 36B4
0.10
0.08
0.06
0.04
0.02
0.00
Ntrk1
Ntrk2
Ntrk3
Ngfr
D
Ntrk1
Ntrk2
Ntrk3
Ngfr
36B4
TGG
DRG
E
TrkB
P75/NGFR
DAPI
TGG
500 µm
F
TrkC
TrkA
DAPI
TGG
500 µm
G
TrkB
P75/NGFR
DAPI
DRG
300 µm
H
TrkC
TrkA
DAPI
DRG
300 µm
I
neurofilament
CGRP
40 µm
J
neurofilament
TrkA
40 µm
K
neurofilament
P75/NGFR
40 µm
L
TrkA
TrkB
TrkC
p75/NGFR
140 kDa
140 kDa
100 kDa
75 kDa
β-actin

Figure 3

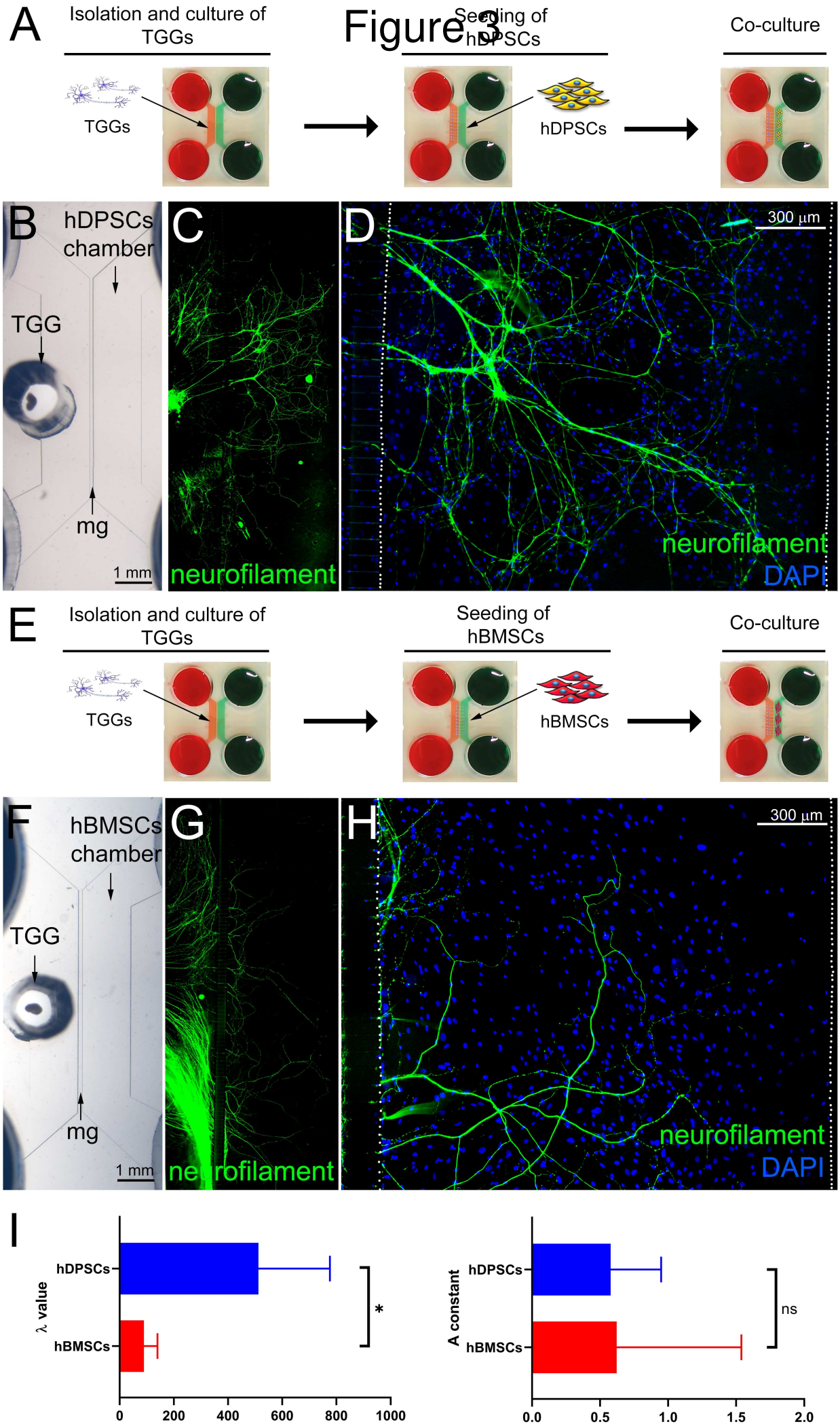
A
Isolation and culture of TGGs
Seeding of hDPSCs
Co-culture
TGGs
hDPSCs
B
hDPSCs chamber
TGG
mg
1 mm
C
neurofilament
D
300 μm
neurofilament
DAPI
E
Isolation and culture of TGGs
Seeding of hBMSCs
Co-culture
TGGs
hBMSCs
F
hBMSCs chamber
TGG
mg
1 mm
G
neurofilament
H
300 μm
neurofilament
DAPI
I
λ value
hDPSCs
hBMSCs
0
200
400
600
800
1000
*
A constant
hDPSCs
hBMSCs
0.0
0.5
1.0
1.5
2.0
ns

Figure 4

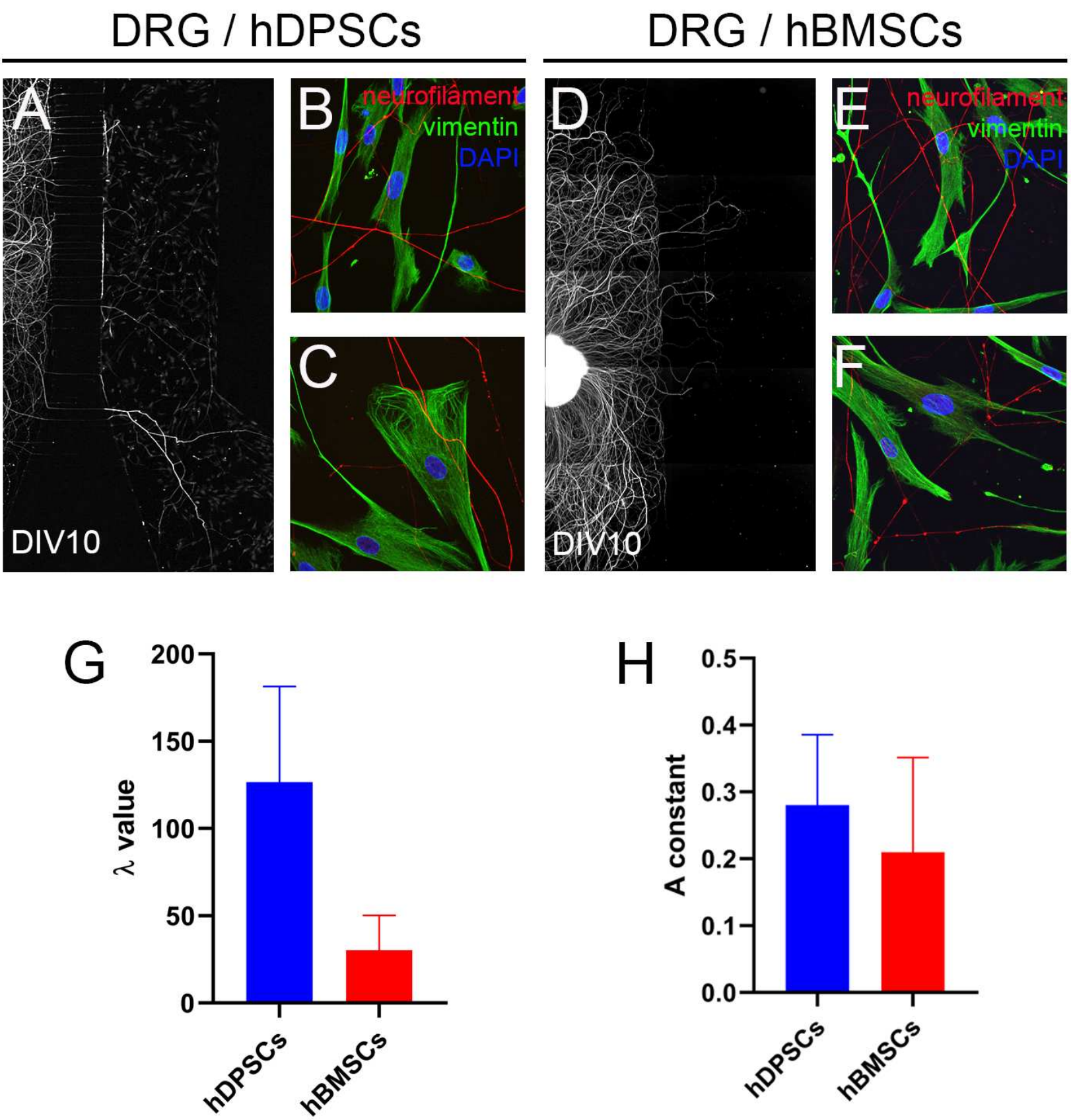
DRG / hDPSCs
DRG / hBMSCs
A
B
neurofilament
vimentin
DAPI
C
D
E
neurofilament
vimentin
DAPI
F
DIV10
DIV10
G
λ value
200
150
100
50
0
hDPSCs
hBMSCs
H
A constant
0.5
0.4
0.3
0.2
0.1
0.0
hDPSCs
hBMSCs

Figure 5

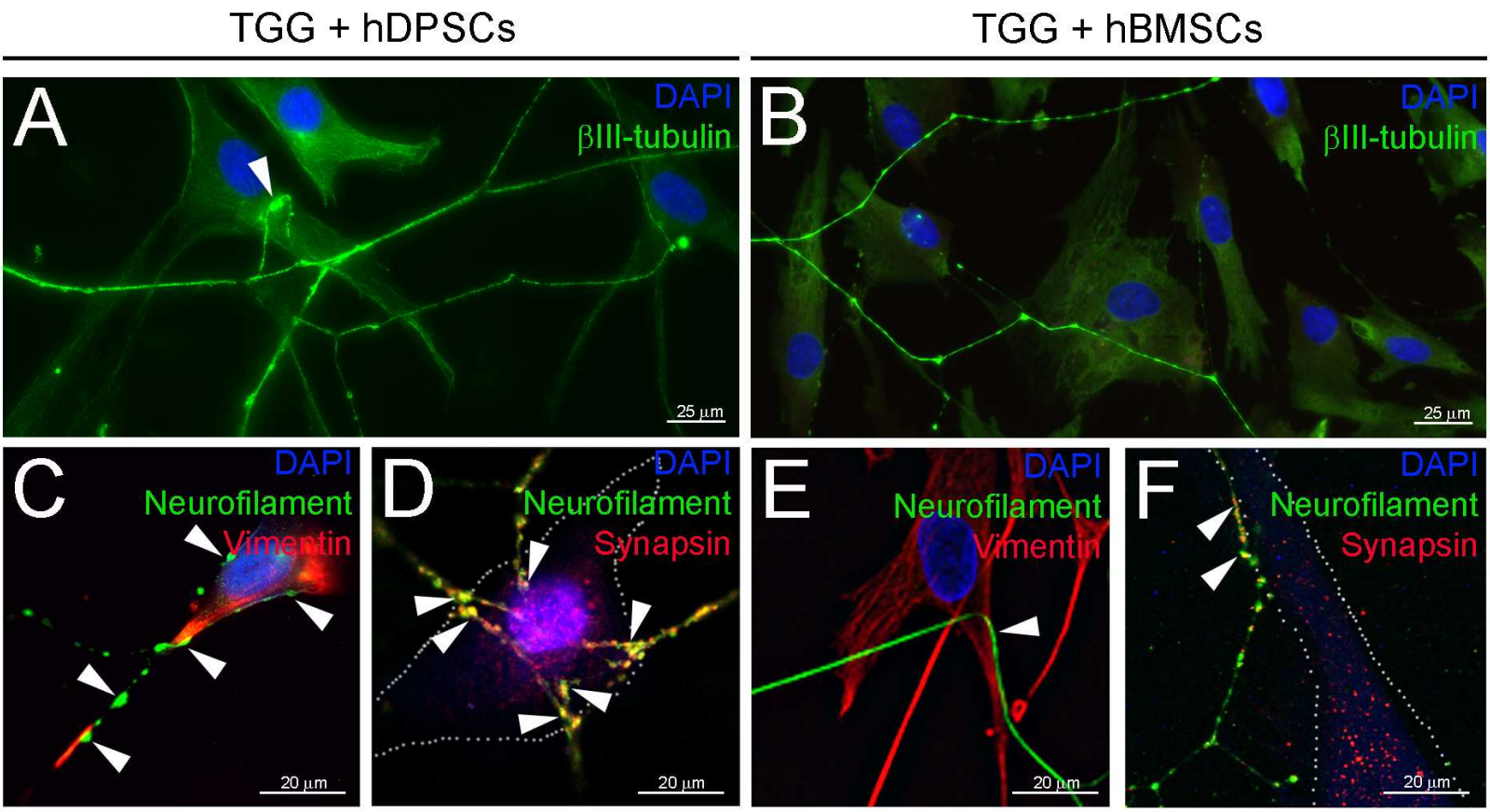
TGG + hDPSCs
TGG + hBMSCs
A
DAPI
βIII-tubulin
25 μm
B
DAPI
βIII-tubulin
25 μm
C
DAPI
Neurofilament
Vimentin
20 μm
D
DAPI
Neurofilament
Synapsin
20 μm
E
DAPI
Neurofilament
Vimentin
20 μm
F
DAPI
Neurofilament
Synapsin
20 μm